

Influences of Pr and Mn co-substitution on crystallinity and electric properties of BiFeO₃ thin films

Takeshi KAWAE,[†] Yuki TERAUCHI, Takashi NAKAJIMA,*
Soichiro OKAMURA* and Akiharu MORIMOTO

College of Science and Engineering, Kanazawa University, Kakuma-machi, Kanazawa, Ishikawa 920-1192

*Department of Applied Physics, Faculty of Science, Tokyo University of Science, 1-3 Kagurazaka, Shinjuku-ku, Tokyo 162-8601

Pr and Mn co-substituted BiFeO₃ (BFO) thin films were fabricated on a Pt-coated (100) SrTiO₃ substrates by pulsed laser deposition (PLD) method. X-ray diffraction patterns indicated that the formation of impurity phases was suppressed by Pr substitution in the BFO thin films. Furthermore, by combining with small amount of Mn substitution, Pr substitution was effective for reducing the leakage current density. The polarization vs electric field curves showed well-saturated hysteresis loops with measurement frequency of 20 kHz at room temperature. The remnant polarization at a maximum electric field of 1500 kV/cm was approximately 50–70 $\mu\text{C}/\text{cm}^2$.

©2010 The Ceramic Society of Japan. All rights reserved.

Key-words : Pb-free materials, BiFeO₃, Pr, Mn, Cosubstitution, Thin films, PLD

[Received April 7, 2010; Accepted June 18, 2010]

1. Introduction

Multiferroic BiFeO₃ (BFO) is well known as a unique material which shows both ferroelectric and ferromagnetic behavior above room temperature because of its high Curie temperature (1123 K) and Neel temperature (653 K).^{1–4)} Simultaneous existence of ferroelectricity and ferromagnetism in a material has attracted scientific and technological attentions for advanced multifunctional devices such as data storage memories, actuators, and sensors. In addition, BFO thin film has a high remnant polarization value in comparison with other ferroelectric materials, and it is known to be an alternative Pb-free ferroelectric material.^{1)–11)} However, the serious problem of BFO thin film is large leakage current at room temperature. In the last several years, many research groups have reported that a site-engineering technique is effective to solve this problem^{12)–33)} because the leakage current of BFO thin films is mainly caused by the nonstoichiometric compositions or impurity phases in the film.^{9)–11)}

On the other hand, in the case of ferromagnetic properties, a small spontaneous magnetization is caused by canting of spin arrangement in BFO.^{1)–4)} Some research groups reported that the rare-earth element or 3d transition metal substitution of BFO showed enhanced ferromagnetic properties due to the modification in the magnetic moments.^{29)–33)} Recently, Yu et al. demonstrated the drastic enhancement of ferromagnetic properties at room temperature due to the increasing the degree of distortion in the BFO by Pr substitution at the Bi-site.³³⁾ Moreover, it can be said that Pr substitution is one of the important techniques to obtain the excellent multiferroic properties of BFO. However, it is not easy to enhance the both ferroelectric and ferromagnetic properties of BFO using the single rare-earth element substitution at Bi-site since the

degradations in ferroelectric properties are caused by excess substitution.^{15)–17)} Thus, it is required to investigate the influences of Pr substitution on the ferroelectric properties of BFO thin films. In our recent works, we have proposed rare-earth element Nd and 3d transition metal Mn co-substituted BFO (BNFM) thin films and succeeded in obtaining improved ferroelectric properties without serious degradations.^{23),24)} Hence, in this paper, we propose Pr and Mn co-substituted BFO (BPFM) and report the crystallinity, ferroelectric and leakage current properties of BPFM thin films by comparing with those of pure and single element-substituted BFO thin films.

2. Experimental procedure

Pr-substituted BFO (BPF) and BPFM thin films were deposited on Pt-coated (100) SrTiO₃ (STO) substrates using a conventional pulsed KrF excimer laser deposition system. The sintered ceramics with compositions of Bi_{1.0}Pr_{0.05}FeO₃ and Bi_{1.0}Pr_xFe_{0.97}Mn_{0.03}O₃ ($x = 0.03, 0.05, 0.07$ and 0.10) were used as targets for BPF and BPFM thin films, respectively. The films were deposited on the substrates at 600°C at an oxygen pressure of 13.3 Pa. After the deposition, the films were annealed at 600°C for 60 min in an oxygen pressure of 2.67 kPa in the same deposition chamber. The thickness of deposited film was approximately 200 nm. Au top electrodes of $2.03 \times 10^{-5} \text{ cm}^2$ in areas were deposited on the films by thermal evaporation using a metal mask to obtain the metal–insulator–metal (MIM) capacitors.

The crystal structure of the films was determined by X-ray diffraction (XRD; Shimadzu XD-D1) analysis with CuK α radiation before the deposition of Au top electrodes. The leakage current of MIM film capacitors was examined with RT-66A (Radiant Technologies). As a ferroelectric property of film capacitors, the polarization vs electric field (P – E) curves were measured by ferroelectric test system (Toyo FCE-1) with a measurement frequency of 0.1–20 kHz. All the measurements were performed at room temperature.

[†] Corresponding author: T. Kawae; E-mail: kawae@ec.t.kanazawa-u.ac.jp

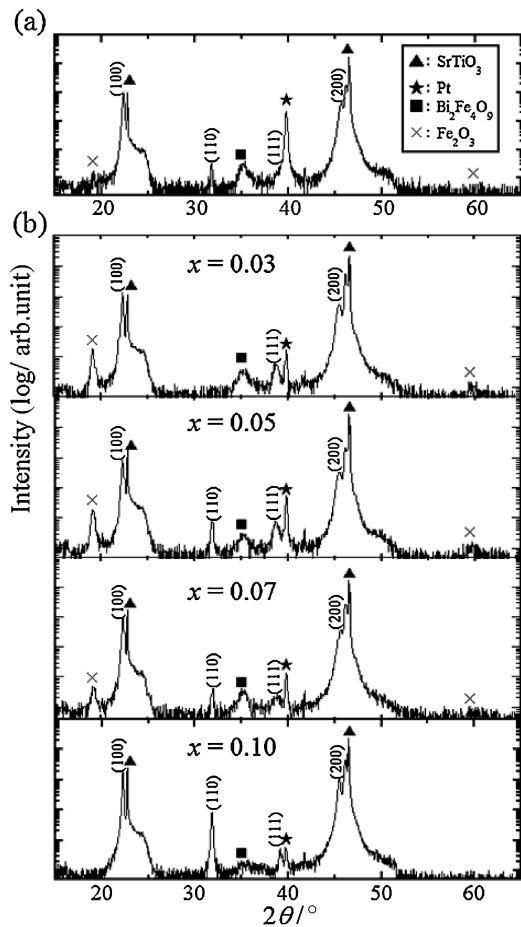


Fig. 1. XRD patterns for (a) BPF and (b) BPFM (Pr concentration $x = 0.03$ – 0.10) thin films grown on the Pt-coated (100) STO substrate. Symbols indicate the impurity phases and substrate.

3. Results and discussions

Figure 1 shows the XRD θ – 2θ scanning patterns of the BPF and BPFM $_{x=0.03-0.10}$ thin films grown on the Pt-coated (100) STO substrates. As shown in the figure, all the BFO thin films are found to be preferentially (100)-oriented on the substrates. On the other hand, as increasing the Pr concentration in the film, the peak intensity of BFO (110) is increased compared with that of BFO (100). In the general PLD process, decreasing the crystallization temperature of deposited materials, ablated particles well migrate on the substrate before crystallization resulting in the highly oriented film grown on the substrate. Hence, we consider this observed behavior is mainly caused by a rise in crystallization temperature of BFO due to the Pr substitution because the similar tendencies have been reported in the rare-earth element substituted BFO thin films.^{23,26} On the other hand, the Bi deficiency phases (such as Bi₂Fe₄O₉ and Fe₂O₃), which was mainly caused by reevaporation of Bi particles from film during deposition process, were observed as shown in the figure although the impurity phases due to Pr excess substitution were not observed even in the 10% Pr-substituted film. In order to investigate the suppression of Bi deficiency phases by the Pr substitution, the peak intensity ratio of Fe₂O₃ (111) to BFO (100) in the films as a function of the Pr concentration in the films is shown in Fig. 2. Here, all the BFO thin films were preferentially (100)-oriented on the substrates since the peak intensity of BFO (100) was higher by approx-

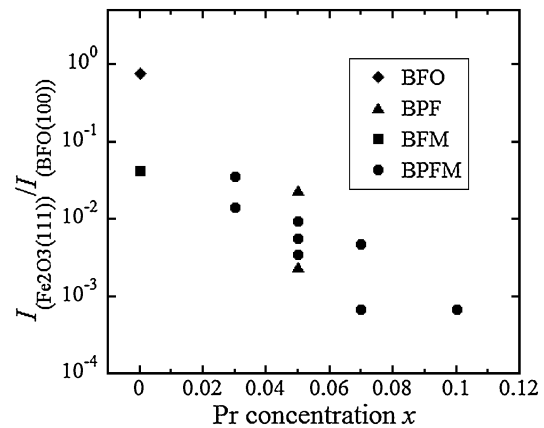


Fig. 2. Normalized peak intensity of Fe₂O₃ (111) as a function of Pr concentration x in the films for the samples shown in Fig. 1.

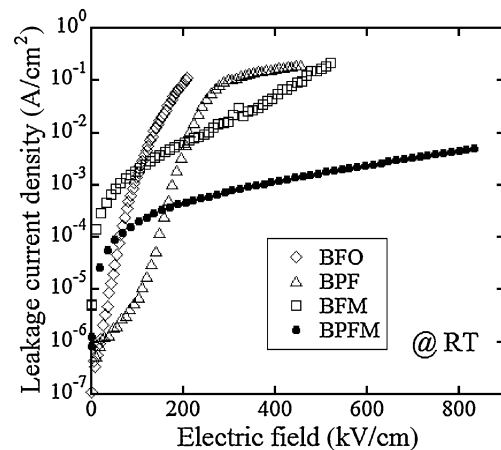


Fig. 3. Leakage current density vs electrical field curves for BFO, BFM, BPF, and BPFM $_{x=0.05}$ film capacitors measured at room temperature.

imately one to two orders of magnitude than those of BFO diffraction peaks with other orientations. We also plotted the results of pure BFO and Mn-substituted BFO (BFM) thin films in the figure.^{23,24} In the Pr-substituted films, the peak intensity ratio is significantly lower than those of BFO and BFM films. The peak intensity of Fe₂O₃ is strongly depressed with increasing the Pr concentration, and the peak almost disappears in the 10% Pr-substituted film (shown in Fig. 1(b)). Other impurity phases due to the Bi deficiency also showed a same tendency. Hence, to obtain the BFO single phase in the film, we suggest that it is effective to substitute the Pr ion at the volatile Bi site of BFO same as reported in the rare-earth elements substituted BFO thin films.^{15,16,23,24,29}

In order to clarify the effects of various dopants, the leakage current properties of fabricated film capacitors at room temperature are shown in Fig. 3. The results of the BFO and BFM thin films were also plotted in the figure.^{23,24} The leakage current density of BPF film is lower than those of other specimens in the low electric field region, but it increases rapidly at an electric field region above 200 kV/cm as shown in the figure. In the BPFM film, the leakage current is not so suppressed as compared with those of other specimens in the low electric field region (<200 kV/cm). However, the remarkable reduced leakage current density is observed in middle to high electric field region (200–850 kV/cm). In order to obtain the excellent ferroelectric

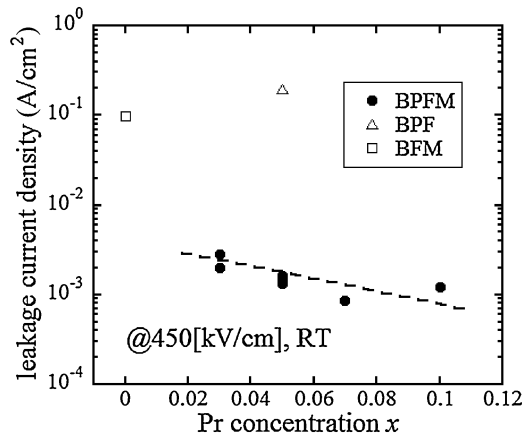


Fig. 4. Leakage current density of film capacitors at 450 kV/cm as a function of Pr concentration x .

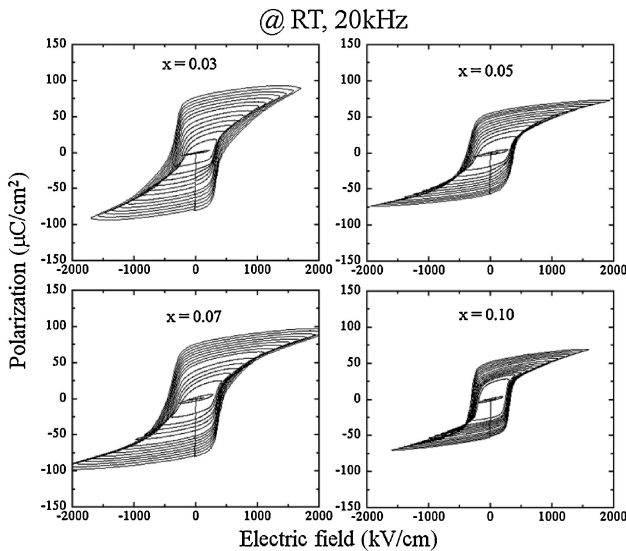


Fig. 5. Polarization vs electrical field curves of BPFM film capacitors (Pr concentration $x = 0.03-0.10$) measured at room temperature with a measurement frequency of 20 kHz.

properties of BFO films, the suppression of leakage current in the high electric field region (above 400 kV/cm) is important because the coercive fields of BFO films are generally 300–500 kV/cm. Hence, it is supposed the Pr and Mn co-substitution is effective technique to reduce the leakage current in the BFO thin films. Also, since the similar behavior in the leakage current property was observed in the Nd and Mn co-substituted BFO thin films, the origin of reduced leakage current in the BPFM thin films might be same as that of BNFM thin films.^{23),24)}

Figure 4 shows the leakage current density at 450 kV/cm as a function of the Pr concentration in the films. As shown in the figure, the leakage current of BPFM thin films are lower by approximately two orders of magnitude than those of single element substituted films. In addition, the leakage current of BPFM film were decreased with increasing the Pr concentration in the films. These results are not only arisen from the suppression of impurity phases shown in Figs. 1 and 2 but also the improvement of surface morphology by the Pr-substitution (not shown in this paper).

Figure 5 shows the $P-E$ curves for the BPFM film capacitors. The $P-E$ curves were measured at room temperature with a

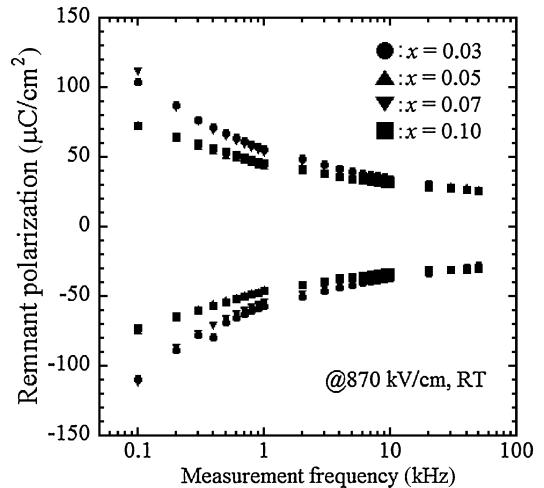


Fig. 6. Dependence of remnant polarization value on the measurement frequency of polarization vs electrical field curves of fabricated BPFM film capacitors (Pr concentration $x = 0.03-0.10$) at the maximum electric field of 870 kV/cm.

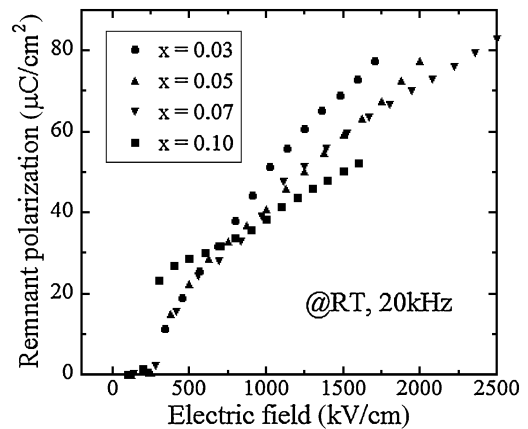


Fig. 7. Electrical field dependence of remnant polarization values measured at room temperature with measurement frequency of 20 kHz for BPFM film capacitor (Pr concentration $x = 0.03-0.10$).

measurement frequency of 20 kHz. For the BPF thin films, the $P-E$ curves are not shown here because of their huge leakage current in the higher bias region than coercive field for BFO thin films (almost 300–400 kV/cm). In the case of BPFM _{$x=0.03$} film, the curve delineates the rounded loops since the suppression of leakage current is not sufficient. Nevertheless, the other specimens ($x > 0.05$) show well-saturated hysteresis loops meaning that both the leakage current and breakdown properties in the film are improved. **Figure 6** shows the dependence of remnant polarization P_r value in the $P-E$ curves of BPFM film capacitors at the maximum electric field of 870 kV/cm on the measurement frequency. As shown in the figure, in the low measurement frequency region from 0.1 to 4 kHz, P_r value was rapidly decreased due to the suppression of leakage current. On the other hand, almost no measurement frequency dependence is found at a high frequency region above 10 kHz. Hence, we conclude that the $P-E$ curves with the measurement frequency of several tens kHz give us the essential ferroelectric properties without influences of leakage current.

Figure 7 shows electric field dependence of remnant polarization for the BPFM film capacitors. The P_r value of films began

to increase at 250–300 kV/cm and monotonically increased with applied electric field up to the electrical breakdown of films (1700–2500 kV/cm). Tendency of saturation in the P_r was still not observed in the highest electric field region. Also, the P_r value at the maximum electric field of 1500 kV/cm were approximately 50–70 $\mu\text{C}/\text{cm}^2$ and were decreased with increasing the substituted Pr concentration as shown in the figure. We suggest that deterioration of P_r value was mainly caused by excess substitution of Pr in the film similar to other rare-earth elements doped BFO thin films,^{15)–17)} and the serious degradations should be avoided by adjusting the amount of substituted Pr ions in the films. This result on the Pr-substitution dependencies of the ferroelectric property suggests a trade-off relationship between the former-mentioned ferromagnetic properties (caused by the increasing the degree of distortion in the BFO by Pr substitution) and the ferroelectric properties. Also, as presented in the Figs. 1 and 2, Pr substitution is effective to obtain the BFO single phase by suppression of the Bi deficiency phases in the film. Therefore, by combining with the investigation of the ferromagnetic properties in the films, it is required to realize the suitable composition of BPFM film which gives us the excellent crystallinity and multiferroic properties.

4. Conclusions

Pr and Mn co-substituted BFO thin films were fabricated on a Pt-coated (100) STO substrates by PLD method. The Pr substitution suppresses the formation of impurity phases caused by the Bi deficiency in the BFO thin films. In the BPFM film capacitors, the suppressions in both impurity phase formation and leakage current were attained. Moreover, the well-saturated P – E hysteresis curves were observed at a measurement frequency of 20 kHz at room temperature. The P_r values for the maximum electric field of 1500 kV/cm were approximately 50–70 $\mu\text{C}/\text{cm}^2$.

Acknowledgements The authors would like to thank Dr. H. Naganuma of Tohoku University, H. Tsuda, F. A. Ali, Y. Nomura and Professor M. Kumeda of Kanazawa University for their technical support and helpful discussions.

References

- 1) J. Wang, J. B. Neaton, H. Zheng, V. Nagarajan, S. B. Ogale, B. Liu, D. Viehland, V. Vaithyanathan, D. G. Schlom, U. V. Waghmare, N. A. Spaldin, K. M. Rabe, M. Wuttig and R. Ramesh, *Science*, **299**, 1719 (2003).
- 2) J. Wang, H. Zheng, Z. Ma, S. Prasertchoug, M. Wuttig, R. Droopad, J. Yu, K. Eisenbeiser and R. Ramesh, *Appl. Phys. Lett.*, **85**, 2574 (2004).
- 3) K. Y. Yun, D. Ricinchi, T. Kanashima and M. Okuyama, *Appl. Phys. Lett.*, **89**, 192902 (2006).
- 4) F. Kubel and H. Schmid, *J. Cryst. Growth*, **129**, 515 (1993).
- 5) J. Li, J. Wang, M. Wuttig, R. Ramesh, N. Wang, B. Ruetter, A. P. Pyatakov, A. K. Zvezdin and D. Viehland, *Appl. Phys. Lett.*, **84**, 5261 (2004).
- 6) S. Y. Yang, F. Zavaliche, L. M. Arbabili, V. Vaithyanathan, D. G. Schlom, Y. J. Lee, Y. H. Chu, M. P. Cruz, Q. Zhan, T. Zhao and R. Ramesh, *Appl. Phys. Lett.*, **87**, 102903 (2005).
- 7) H. Naganuma and S. Okamura, *J. Appl. Phys.*, **101**, 09M103 (2007).
- 8) S. K. Singh and H. Ishiwara, *Jpn. J. Appl. Phys.*, **44**, L734 (2005).
- 9) K. Y. Yun, M. Noda, M. Okuyama, H. Saeki, H. Tabata and K. Saito, *J. Appl. Phys.*, **96**, 3399 (2004).
- 10) H. Y. Go, N. Wakiya, H. Funakubo, K. Satoh, M. Kondo, J. S. Cross, K. Maruyama, N. Mizutani and K. Shiosaki, *Jpn. J. Appl. Phys.*, **46**, 3491 (2007).
- 11) H. Bae, M. Bibes, A. Barthelemy, K. Bouzehouane, E. Jacquet, A. Khoda, J.-P. Contour, S. Fushi, F. Wyczisk, A. Forget, D. Lebeugle, D. Colson and M. Viret, *Appl. Phys. Lett.*, **87**, 072508 (2005).
- 12) T. Kawae, Y. Teuchi, H. Tsuda, M. Kumeda and A. Morimoto, *Appl. Phys. Lett.*, **94**, 112904 (2009).
- 13) S. Yasui, H. Uchida, H. Nakaki, K. Nishida, H. Funakubo and S. Koda, *Appl. Phys. Lett.*, **91**, 022906 (2007).
- 14) S. K. Singh, H. Ishiwara and K. Maruyama, *Appl. Phys. Lett.*, **88**, 262908 (2006).
- 15) H. Uchida, R. Ueno, H. Funakubo and S. Koda, *Jpn. J. Appl. Phys.*, **44**, L561 (2005).
- 16) H. Uchida, R. Ueno, H. Funakubo and S. Koda, *J. Appl. Phys.*, **100**, 014106 (2006).
- 17) G. D. Hu, X. Cheng, W. B. Wu and C. H. Yang, *Appl. Phys. Lett.*, **91**, 232909 (2007).
- 18) Y. H. Lee, J. M. Wu and C. H. Lai, *Appl. Phys. Lett.*, **88**, 042903 (2006).
- 19) Y. P. Liu and J. M. Wu, *Electrochem. Solid-State Lett.*, **10**, G39 (2007).
- 20) F. Huang, X. Lu, W. Lin, X. Wu, Y. Kan and J. Zhu, *Appl. Phys. Lett.*, **89**, 242914 (2006).
- 21) J. K. Kim, S. S. Kim, W. J. Kim, A. Bhalla and R. Guo, *Appl. Phys. Lett.*, **88**, 132901 (2006).
- 22) X. Qi, J. Dho, R. Tomov, M. Blamire and J. L. MacManus-Driscoll, *Appl. Phys. Lett.*, **86**, 062903 (2005).
- 23) T. Kawae, H. Tsuda and A. Morimoto, *Appl. Phys. Express*, **1**, 051601 (2008).
- 24) T. Kawae, H. Tsuda, H. Naganuma, S. Yamada, M. Kumeda, S. Okamura and A. Morimoto, *Jpn. J. Appl. Phys.*, **47**, 7586 (2008).
- 25) S. K. Singh, K. Maruyama and H. Ishiwara, *Appl. Phys. Lett.*, **91**, 112913 (2007).
- 26) C. C. Lee and J. M. Wu, *Electrochem. Solid-State Lett.*, **10**, G58 (2007).
- 27) Z. Cheng, X. Wang, S. X. Dou, H. Kimura and K. Ozawa, *Phys. Rev. B*, **77**, 092101 (2008).
- 28) S. K. Singh, H. Ishiwara, K. Sato and K. Maruyama, *J. Appl. Phys.*, **102**, 094109 (2007).
- 29) Z. X. Cheng, X. L. Wang, S. X. Dou, H. Kimura and K. Ozawa, *J. Appl. Phys.*, **104**, 116109 (2008).
- 30) Z. Quan, W. Liu, H. Hu, S. Xu, B. Sebo, G. Fang, M. Li and X. Zhao, *J. Appl. Phys.*, **104**, 084106 (2008).
- 31) H. Naganuma, J. Miura and S. Okamura, *Appl. Phys. Lett.*, **93**, 052901 (2008).
- 32) M. Azuma, H. Kanda, A. A. Belik, Y. Shimakawa and M. Takano, *J. Magn. Magn. Mater.*, **310**, 1177 (2007).
- 33) B. Yu, M. Li, Z. Hu, L. Pei, D. Guo, X. Zhao and S. Dong, *Appl. Phys. Lett.*, **93**, 182909 (2008).